PARTEC 2007

From weak powders to strong solids – tension tests

S. Luding[1], I. Kadashevich[1]

[1)] Particle Technology, Nanostructured Materials, DelftChemTech, TUDelft, Julianalaan 136, 2628 BL Delft, Netherlands, s.luding@tudelft.nl, i.kadashevich@tudelft.nl

ABSTRACT

The contacts between cohesive, frictional particles with a few μm in size are studied. Discrete Element Model (DEM) simulations rely on realistic contact force models: A rather simple, objective contact model is used, involving the physical properties of elastic-plastic repulsion, dissipation, adhesion, friction as well as rolling- and torsion-resistance. Bulk properties like friction, cohesion and yield-surfaces, can be modeled, but here, tensile strength tests after pressure-sintering are presented for different contact adhesion strength. The tensile strength increases with contact adhesion, but kinetic energy, coordination number and density decrease.

INTRODUCTION

Contacts between cohesive, frictional particles with sizes in the size-range of micrometers are modeled with the Discrete Element Model (DEM) Such cohesive, frictional, fine powders show a peculiar flow behavior that can be quantified by macroscopic bulk properties as, among others, cohesion, friction, yield- or tensile-strength, dilatancy, stiffness, and anisotropy. Furthermore, the propagation of information in granular media is an issue to be understood, especially if adhesion, friction, and other contact mechanisms are involved (Luding, 2005, Mouraille 2006).

The “microscopic” contact forces and torques control the macroscopic bulk properties (Vermeer, 2001). A Discrete Element Model (DEM) requires the contact forces and torques as the basic input, to solve the equations of motion for all particles in a granular system (Allen, 1987). Research challenges involve not only the realistic DEM simulations of many-particle systems and their experimental validation, but also the transition from the microscopic contact properties to the macroscopic flow behavior. In this study, a minimal set of contact models (and parameters) (Tomas, 2001, Luding, 2001, Luding, 2006, Luding, 2007) allows to simulate various modes of bulk behavior, i.e., both compressive and tensile failure.

The model allows for pressure-sintering: A sample of particles can be compressed and then forms a solid block. The solid then is examined by both a compressive and a tensile test -- and all this without advanced modeling of non-spherical particles and without the typically used beam-like models for contact adhesion and rolling resistance (d’Addetta, 2006)

SIMULATION MODEL

Many-particle simulations methods like DEM can complement experiments on rather small ``representative volume elements'' (REVs), by providing deeper and more detailed insight into the kinematics and dynamics of the powders examined. Large scale industrial applications, simulated particle by particle, are out of reach of DEM, since much more than the typical easy-to-deal-with million particles are involved in a silo or a dam.

The particles a powder consists of, generally deform under stress. A realistic modeling of the deformations of particles in contact with each other is by far too great a task if thousands of particles are involved. Therefore, the normal interaction forces are related to the overlap of two particles, see Fig.1.

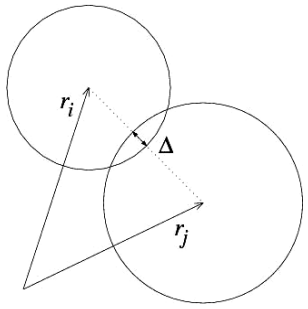

Figure 1: Two particle contact with overlap Δ.

In tangential direction, forces and torques also depend on the tangential displacement and the relative rotations of the particle surfaces – different rotational degrees of freedom are responsible for sliding, rolling and torsion. Given

the sum of forces acting on a particle, either from other particles, or from walls, the problem is reduced to the integration of Newton's equations of motion for the translational and rotational degrees of freedom (Allen and Tildesley, 1987). The typically short-ranged interactions in granular media, allow for optimization by using linked-cell (LC) or alternative methods in order to make the neighborhood search more efficient. In the case of long-range interactions, (e.g., charged particles or van der Waals type forces) this is not possible anymore, so that more advanced methods for speed-up have to be applied.

In this study, two spherical particles interact only if they are in contact. The force acting on a given particle from another at contact c, can be decomposed into a normal and a tangential part. The tangential force leads to a torque – like rolling and torsion do – but rolling and torsion do not affect the translational degrees of freedom (Luding, 2007). The simplest normal contact force model, which takes care of excluded volume, and thus the particle elasticity and stiffness, as well as dissipation, involves a linear repulsive and a linear viscous (velocity-dependent) force with a spring stiffness and a viscous damping. This so-called linear spring dashpot (LSD) model describes particle contact as a damped harmonic oscillator, for which the half-period of a vibration around an equilibrium position with a certain contact force, can be computed analytically (Luding, 1998). Below, a variant of the linear, hysteretic spring model is used, a simpler version of more advanced models, see (Luding, 2007) and references therein.

MODEL SYSTEM AND SINTERING

In this section, a uni-axial tension test is presented. Before the deformations can be applied, the sample of lose powder first has to be pressure sintered, then stress-relaxed, and eventually tension or compression tests can be performed. The contact model and the parameters used are introduced and discussed in (Luding, 2007). If particle-particle contacts are different from particle-wall contacts, this will be explicitly stated.

The system contains N=1728 particles with radii a_i drawn from a Gaussian distribution around mean a=0.005mm (David, 2005, Luding, 2007). The volume fraction $\nu=\Sigma\, V(a_i)/V$ reached during the pressure sintering with p_s=10 is ν=0.675, with the particle volume $V(a_i)=(4/3)\pi a_i^3$, and the coordination number is C=7.16 in this state. After stress-relaxation, these values have changed to ν=0.630 and C=6.23. A different preparation procedure (with adhesion k_c/k_2=1/2 during sintering) does not lead to a markable difference in density after sintering. However, one observes ν=0.629 and C=6.19 after relaxation. For both preparation procedures the tension results are practically identical, so that only the first procedure is presented in the following.

For *pressure sintering*, a lose assembly of particles is first compressed with an isotropic stress p_s in a cuboid volume. This way, the plastic deformation and thus the adhesive contact forces are active. Two of the six walls are strongly adhesive from the beginning so that the sample sticks to them, while all other walls (and also the particles among themselves) are adhesionless, so that the side-walls can be easily removed in the second phase. All walls are frictionless during sintering, while the particles are slightly frictional. Pressure sintering is stopped when the kinetic energy of the sample is many orders of magnitude smaller than the potential energy.

During *stress-relaxation*, all wall stresses are released to 0.1% of the sintering stress. Thus, the non-adhesive side-walls still feel a very small stress that keeps them close to the sample, for convenience. For tension (compression), one of the two sticky walls is slowly and smoothly moved outwards (inwards), like described in earlier studies, following a prescribed cosine-function with time (Luding, 2004, Luding 2004b).

The particle-wall contact parameters are the same, except for adhesion and friction, for which 20 and 10 times larger values are used, respectively, the former during all stages, the latter only during tensile testing. The choice of numbers and units is such that the particles correspond to around five micro-meter sized spheres.

TENSION TESTS

The tensile tests are performed uni-axially in x-direction by increasing slowly and smoothly the distance between the two sticky walls. (The same initial sample, prepared with k_c/k_2=0, is used for all tests reported here.) The stress-strain curves for different cohesion are plotted in Fig. 1.

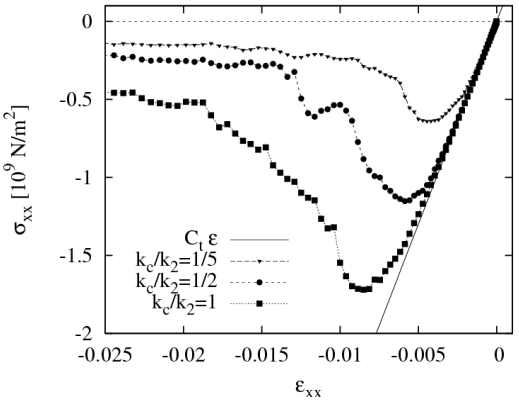

Fig.1: Axial tensile stress plotted against tensile strain for simulations with weak, moderate and strong particle contact adhesion; the k_c/k_2 ratios are given in the inset. The line gives a fit to thelinear elastic regime with slope 2.6 10^{11} N/m.

The axial tensile stress initially increases linearly with strain, practically independent from the contact adhesion strength. With increasing strain a considerable number of contacts are opened due to tension, see Fig. 2. The contacts open more easily and more rapidly for smaller adhesion. This leads to a decrease of the stress-strain slope before the stress reaches a maximum and the sample turns into a softening failure mode. As expected, the maximal stress is increasing with contact adhesion k_c/k_2, and a larger adhesion force allows for larger deformation before failure. The compressive strength is 6-7 times larger (Luding, 2007) – data not shown.

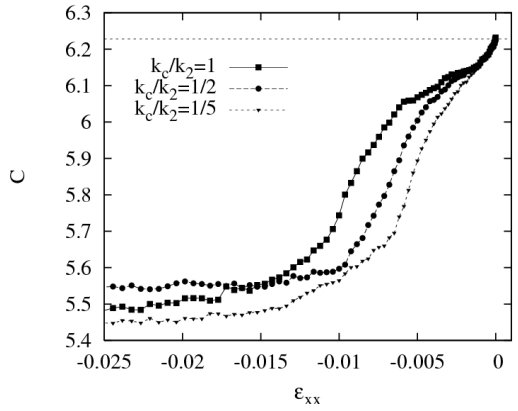

Fig.2: Coordination number (contacts per particle) plotted against tensile strain for the same simulations as shown in Fig. 1. Note that this is a global average: the C values in the failure zone are considerably smaller while those in the remaining stable solid remain close to the initial value.

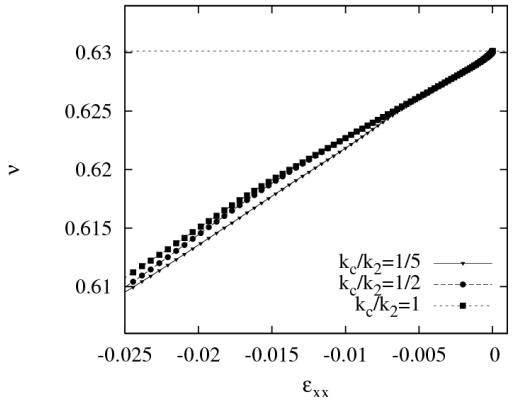

Fig.3: Volume fraction, during the tensile test with weak side stress (data not shown), plotted against tensile strain for the same simulations as shown in Fig. 1.

The density (volume fraction, see Fig.3) decreases continuously during tension and stronger contact adhesion leads to slightly larger densities at comparable levels of tension.

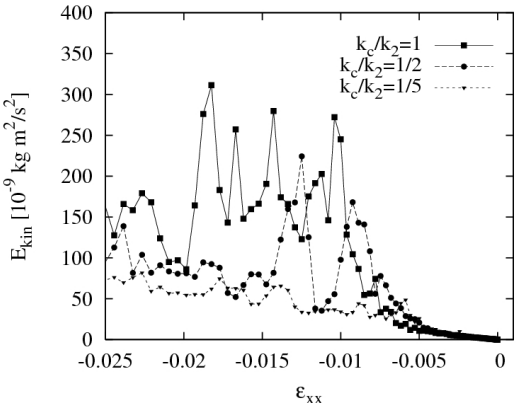

Fig.4: Kinetic energy plotted against tensile strain for the same simulations as shown in Fig. 1.

The kinetic energy, see Fig.4, increases slowly during tension. Only after failure/softening, bursts of the kinetic energy indicate the dynamic nature of the failure modes. Stronger contact adhesion leads to larger and longer enduring bursts of kinetic energy.

SUMMARY AND CONCLUSIONS

The behavior of a sintered solid (made from about 2000 primary particles) is modeled when subject to tension, using a discrete element method with a special contact model, involving

elastic-visco-plastic normal contact forces, adhesion, friction, and rolling- as wellas torsion resistance -- all in one.

The powder-sample is first pressure-sintered, then the wall-stress is released and finally, the sample is subject to strain-controlled tension until it fails – and further on. Stronger contact adhesion leads to considerably larger strength, but not to larger (elastic) moduli. The effect of sliding-friction, rolling- and torsion-resistance is weak as compared to the effect contact adhesion (Luding, 2007).

A more quantitative tuning of the present DEM model to real experimental data remains a challenge for the future. The fine-adjustement will require a much more systematic study of all other contact model parameters.

ACKNOWLEDGEMENTS

The authors acknowledge support from the Delft Centre for Materials (DCMat), the Deutsche Forschungsgemeinschaft (DFG), and FOM (Fundamenteel Onderzoek der Materie), financially supported by the Nederlandse Organisatie voor Wetenschappelijk Onderzoek (NWO). Many helpful discussions with A. Suiker and L. Brendel are acknowledged.

REFERENCES

1. Allen M. P. & Tildesley D. J., (1987), Computer simulation of liquids, Oxford University Press Inc., New York.
2. D'Addetta, G. A., Kun, F., Ramm, E., (2002) *On the application of a discrete model to the fracture process of cohesive granular materials*, Granular Matter 4 (2), 77-90.
3. David, C. T., Garcia-Rojo, R., Hermann, H. J., and Luding, S. (2005), *Hysteresis and Creep in Powders and Grains*, in: Powders and Grains 2005, Eds. R. Garcia Rojo, S. McNamara, and H. J. Herrmann, Balkema.
4. Herrmann, H. J., Hovi, J.-P., and Luding, S., eds. (1998) *Physics of dry granular media*, NATO ASI Series E 350, Kluwer Academic Publishers, Dordrecht.
5. Luding, S., and Herrmann, H. J. (2001), *Micro-Macro Transition for Cohesive Granular Media*, in: Zur Beschreibung komplexen Materialverhaltens, Institut für Mechanik, S. Diebels (Ed.), Stuttgart, 121.
6. Luding, S. (2004), *Micro-macro transition for anisotropic, frictional granular packings*. Int. J. Sol. Struct. 41, 5821-5836.
7. Luding S. (2004b), *Molecular dynamics simulations of granular materials*. In H. Hinrichsen and D. E. Wolf (Eds.), The Physics of Granular Media, Wiley VCH, Weinheim, Germany, pp 299-324.
8. Luding, S. (2005), *Granular Media – Information propagation*. Nature 435 (7039) 159.
9. Luding, S. (2006), *About contact laws for frictional granular particles*. In: Behavior of Granular Media (research report).
10. Luding, S. (2007), *Tensile tests with new contact laws for frictional granular particles*. submitted to Granular Matter.
11. Mouraille, O., Mulder, W. A., Luding, S. (2006), Sound wave acceleration in Granular Materials. JSTAT, P07023.
12. Thornton, C., and Antony, S. J. (2000), *Quasi-static deformation of a soft particle system*, Powder Technology 109(1-3), 179-191.
13. Tomas, J. (2001), *Assessment of mechanical properties of cohesive particulate solids – part 1: particle contact constitutive model*, Part. Sci. Technol. 19, 95-110.
14. Vermeer, P. A., Diebels, S., Ehlers, W., Herrmann, H. J., Luding, S., and Ramm, E., eds., *Continuous and Discontinuous Modelling of Cohesive Frictional Materials*, Lecture Notes in Physics 568, Springer, Berlin, 2001